

A. Ekström,<sup>1</sup> J. Cederkäll,<sup>1,2</sup> C. Fahlander,<sup>1</sup> M. Hjorth-Jensen,<sup>3</sup> F. Ames,<sup>4</sup> P. A. Butler,<sup>5</sup> T. Davinson,<sup>6</sup> J. Eberth,<sup>7</sup> F. Fincke,<sup>7</sup> G. Georgiev,<sup>2</sup> A. Gorgen,<sup>8</sup> M. Górska,<sup>9</sup> D. Habs,<sup>10</sup> A. M. Hurst,<sup>5</sup> M. Huyse,<sup>11</sup> O. Ivanov,<sup>11</sup> J. Iwanicki,<sup>12</sup> O. Kester,<sup>9</sup> U. Köster,<sup>2</sup> B. A. Marsh,<sup>13,14</sup> J. Mierzejewski,<sup>12</sup> O. Niedermaier,<sup>15</sup> P. Reiter,<sup>7</sup> H. Scheit,<sup>15</sup> D. Schwalm,<sup>15</sup> S. Siem,<sup>16</sup> G. Sletten,<sup>17</sup> I. Stefanescu,<sup>11</sup> G. M. Tveten,<sup>2,16</sup> J. Van de Walle,<sup>11</sup> P. Van Duppen,<sup>2</sup> D. Voulot,<sup>14</sup> N. Warr,<sup>7</sup> D. Weisshaar,<sup>7</sup> F. Wenander,<sup>14</sup> and M. Zielinska<sup>12</sup>

<sup>1</sup>*Physics Department, University of Lund, Box 118, SE-221 00 Lund, Sweden*

<sup>2</sup>*PH Department, CERN 1211, Geneva 23, Switzerland*

<sup>3</sup>*Physics Department and Center of Mathematics for Applications, University of Oslo, Norway*

<sup>4</sup>*TRIUMF, Vancouver, Canada*

<sup>5</sup>*Oliver Lodge Laboratory, University of Liverpool, United Kingdom*

<sup>6</sup>*Department of Physics and Astronomy, University of Edinburgh, United Kingdom*

<sup>7</sup>*Institute of Nuclear Physics, University of Cologne, Germany*

<sup>8</sup>*CEA Saclay, DAPNIA/SPhN, Gif-sur-Yvette, France*

<sup>9</sup>*Gesellschaft für Schwerionenforschung, Darmstadt, Germany*

<sup>10</sup>*Physics Department, Ludwig-Maximilian University, Munich, Germany*

<sup>11</sup>*Instituut voor Kern- en Stralingsfysica, K.U. Leuven, Belgium*

<sup>12</sup>*Heavy Ion Laboratory, Warsaw University, Poland*

<sup>13</sup>*Department of Physics, University of Manchester, United Kingdom*

<sup>14</sup>*AB Department, CERN 1211, Geneva 23, Switzerland*

<sup>15</sup>*Max-Planck Institute of Nuclear Physics, Heidelberg, Germany*

<sup>16</sup>*Department of Physics, University of Oslo, Norway*

<sup>17</sup>*Physics Department, University of Copenhagen, Denmark*

(Dated: February 5, 2008)

The reduced transition probabilities,  $B(E2; 0_{\text{gs}}^+ \rightarrow 2_1^+)$ , have been measured in the radioactive isotopes  $^{108,106}\text{Sn}$  using sub-barrier Coulomb excitation at the REX-ISOLDE facility at CERN. Deexcitation  $\gamma$  rays were detected by the highly segmented MINIBALL Ge-detector array. The results,  $B(E2; ^{108}\text{Sn}) = 0.222(19)e^2b^2$  and  $B(E2; ^{106}\text{Sn}) = 0.195(39)e^2b^2$  are  $\sim 30\%$  larger than shell-model predictions and deviate from the generalized seniority model. This experimental result may point towards a weakening of the  $N = Z = 50$  shell closure.

PACS numbers: 23.20.Js, 21.60.Cs, 25.70.De, 27.60.+j

One of the pressing questions in nuclear physics today is whether the shell closures that are well established close to  $\beta$ -stability remain so also for isotopes with a more extreme proton-to-neutron ratio. Newly developed facilities that produce well-focussed radioactive ion beams now make it possible to address this issue experimentally. One approach to this question is to measure the reduced transition probabilities – the  $B(E2; 0_{\text{gs}}^+ \rightarrow 2_1^+)$  – for specific nuclei in the vicinity of the shell-closure under study. In the case at hand here, the  $^{100}\text{Sn}$  shell closure, it is consequently of significant interest to determine this  $B(E2)$  in the sequence of neutron deficient even-mass Sn isotopes. Recent measurements of this quantity in  $^{110,108}\text{Sn}$  [1–3] consistently deviate from the broken-pair model as given by the generalized seniority scheme [4] and from large-scale shell-model calculations [1]. Parallel work [3], to what we present here, using intermediate energy Coulomb excitation suggests a constant trend of the reduced transition probabilities extending to  $^{106}\text{Sn}$ . Such a trend is at variance with the seniority model. In this paper we report results from the first measurements of  $^{108,106}\text{Sn}$  using sub-barrier Coulomb excitation. This is the only experiment so far for  $^{106}\text{Sn}$  that has allowed for complete control of the scattering process and thus

explicitly fulfills the conditions for safe Coulomb excitation. Our result still deviates significantly from theoretical predictions but indicates a decreasing trend of the  $B(E2)$  with a decreasing number of valence particles outside of the  $^{100}\text{Sn}$  core. It has been suggested that the current disagreement between published results and model prediction could possibly be attributed to experimental normalization effects [5]. For this reason we note that with this paper three different normalization methods have been used, all yielding similar results for  $^{110,108}\text{Sn}$ . Thus, it appears that the difference between theory and observation is of physical origin. In conclusion, the seniority model describes the structural evolution of the neutron-rich Sn isotopes well but as the structure becomes dominated by the  $\nu(0g_{7/2}1d_{5/2})$  orbits this interpretation appears to break down.

The experiment was carried out at the REX-ISOLDE [6] facility at CERN. The radioactive beams were produced by bombarding a  $27 \text{ g/cm}^2$   $\text{LaC}_x$  primary target by 1.4 GeV protons delivered by the CERN PS Booster. Atomic Sn was singly ionized using a resonant three-step laser scheme and subsequently extracted by an electric potential. Beams with mass numbers  $A=108$  or  $A=106$  were selected by electromagnetic separation using the General

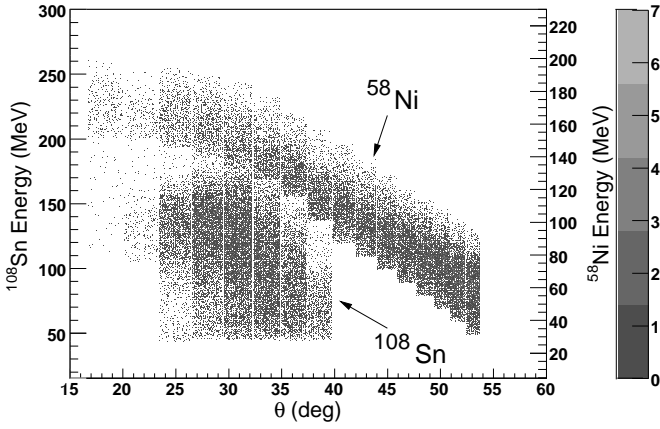


FIG. 1: Energy and angle of the scattered beam and target particles as detected by the DSSSD. The kinematical cuts used to distinguish between ejectiles and recoils are imposed. The corresponding plot for the  $^{106}\text{Sn}$  case is similar.

Purpose Separator of the facility. The half-lives of  $^{108}\text{Sn}$  and  $^{106}\text{Sn}$  are 10.30(8) min and 115(5) s [7], respectively. The beam was charge bred for 67 ms in an electron beam ion source [8] in order to reach the  $26^+$  charge state used for post-acceleration. The final energy was 2.82 and 2.83 MeV/u for the  $A=108$  and  $A=106$  beams, respectively. This is well below the safe bombarding energy [9] of  $\sim 3.6$  MeV/u, assuming a safe distance of 5 fm. The  $2 \text{ mg/cm}^2$   $^{58}\text{Ni}$  target was isotopically enriched to 99.9%. The first excited  $2^+$  state in  $^{58}\text{Ni}$ , used for normalization, is located at 1454 keV, and has an adopted  $B(E2; 0_{\text{gs}}^+ \rightarrow 2_1^+) = 0.0705(18) \text{ e}^2\text{b}^2$  given by ENSDF [7]. Emitted  $\gamma$  rays were registered in the MINIBALL [10] detector array which surrounds the target in a close to  $4\pi$  configuration. Energy and scattering angle of ejectiles and recoils were detected by a pixelated circular double sided silicon strip detector (DSSSD) [11] placed 30 mm downstream from the target (Fig. 1). Data were recorded using two trigger conditions. The first one was activated by particle- $\gamma$  coincidence events with a time window of 800 ns and the second one by events arising from one or more particles detected in the DSSSD. The latter trigger was downscaled by a factor of  $2^6$ . Ejectiles and recoils were easily separated due to the inverse kinematics and mass difference between target and beam particles. In brief, the results presented in this paper were obtained with the following conditions on the data:

- Coincident particle- $\gamma$  events.
- Kinematical separation of ejectiles and recoils.
- Selection of  $2p$  events and kinematical reconstruction using  $1p$  events.

Figure 2 shows the Coulomb excitation  $\gamma$ -rays peaks in the spectrum after imposing the analysis conditions and correcting for Doppler broadening. The lasers were

switched on and off with 14.4 s intervals for one hour every three hours throughout the experiments in order to measure the composition of the scattered beam over time. Using this information, in combination with the constant cross section for the Coulomb excitation of the contaminants, the respective Sn fractions could be determined over the full duration of the experiments and were 59.0(27)% and 29.2(42)% for the  $^{108}\text{Sn}$  and  $^{106}\text{Sn}$  beams, respectively. Moreover, the linear correlation coefficient between the laser power and the number of detected  $^{108}\text{Sn}$  particles were also determined and was 0.90. This allowed for a consistency check of the  $^{108}\text{Sn}$  content of beam. Details regarding the data analysis will be published in a forthcoming paper [12]. The  $B(E2)$  values were extracted from the experimental data using the coupled-channels Coulomb excitation code GOSIA2 [13]. One should note that the static quadrupole moment  $Q(2_1^+)$  in  $^{112}\text{Sn}$  is consistently 0 b [14]. For this reason a  $Q(2_1^+) = 0$  b was used also in the current analysis. Input parameters and results are displayed in Tab. I and in Figs. 2 and 3. These results deviate from the

TABLE I: The two rightmost columns give background information as well as results for the two cases discussed in the text. The Coulomb excitation yields were extracted from the bin content of the relevant peaks. The last row gives the resulting  $B(E2)$  values.

Data	$A = 108^a$	$A = 106^b$
$E(2^+)$ [keV]	1206	1206
Bin $I_\gamma$ (Ni)	576.5(335)	206.5(149)
Bin $I_\gamma$ (Sn)	994.0(383)	132.5(144)
FWHM(Sn) [keV]	19.3(8)	22.5(26)
FWHM(Ni) [keV]	33.1(18)	26.5(24)
$B(E2; \uparrow)$ [ $\text{e}^2\text{b}^2$ ]	0.222(19)	0.195(39)

<sup>a</sup>2.82 MeV/u  $^{108}\text{Sn}$  on 2.0 mg/cm<sup>2</sup>  $^{58}\text{Ni}$ .

<sup>b</sup>2.83 MeV/u  $^{106}\text{Sn}$  on 2.0 mg/cm<sup>2</sup>  $^{58}\text{Ni}$ .

theoretical prediction by more than  $1\sigma$ . As mentioned, according to the seniority model the  $B(E2)$  values naturally decrease with a decreasing number of particles outside the closed core. This trend can be noted in our data (Fig. 3) especially for  $^{106}\text{Sn}$ . The significance of the current results can be understood as follows. The relative uncertainty for our  $^{108}\text{Sn}$  and  $^{106}\text{Sn}$  measurements are 8.6% and 20.0%, respectively. The uncertainty for the  $^{108}\text{Sn}$  measurement reported in Ref. [1] was 24.8% whereas the corresponding total uncertainty for the of  $^{108}\text{Sn}$  and  $^{106}\text{Sn}$  measurements in Ref. [3] was 17.0% and 24.3%. Taking the weighted mean between our result and the two aforementioned  $^{108}\text{Sn}$  measurements gives a  $B(E2; 0_{\text{gs}}^+ \rightarrow 2_1^+) = 0.224 \pm 0.016 \text{ e}^2\text{b}^2$ , i.e. a relative error of 7.1%. Similarly, the weighted mean between our result and the single measurement of Ref. [3] for  $^{106}\text{Sn}$  gives a  $B(E2; 0_{\text{gs}}^+ \rightarrow 2_1^+) = 0.209 \pm 0.032 \text{ e}^2\text{b}^2$ , i.e. a relative error of 14.3%. We again note that the present experiment for  $^{106}\text{Sn}$  is currently the only one to explicitly fulfill the safe condition.

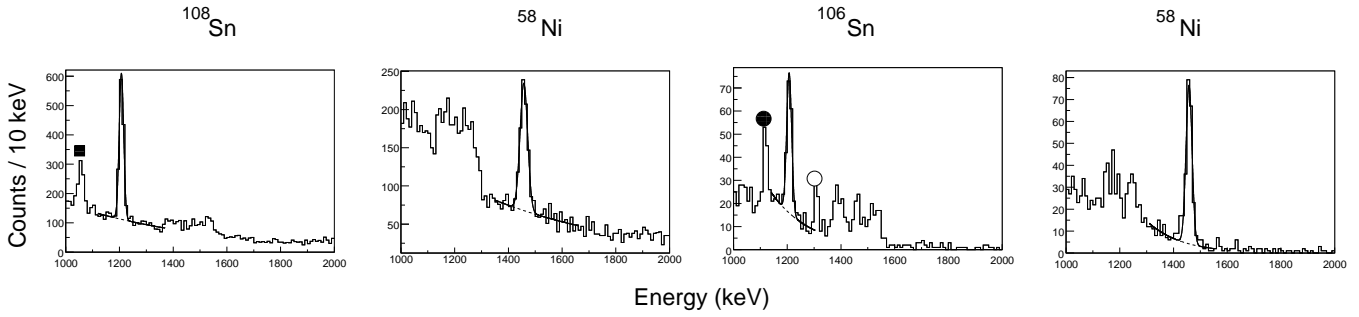


FIG. 2:  $2p + 1p$  Doppler corrected  $\gamma$ -ray spectra from the  $^{108}\text{Sn}$  and  $^{106}\text{Sn}$  experiments. The peak indicated by  $\blacksquare$  comes from two closely located  $^{108}\text{In}$  decay  $\gamma$ -rays that merge due to Doppler correction. The  $\gamma$ -ray marked with  $\bullet$  is the deexcitation from the  $8^+$  state at 1117.8(2) keV to the  $7^+$  ground state in  $^{106}\text{In}$  [15]. Similarly the  $\gamma$ -ray marked with  $\circ$  is the deexcitation from the  $9^+$  state at 1307.08(7) keV to the ground state in the same nucleus.

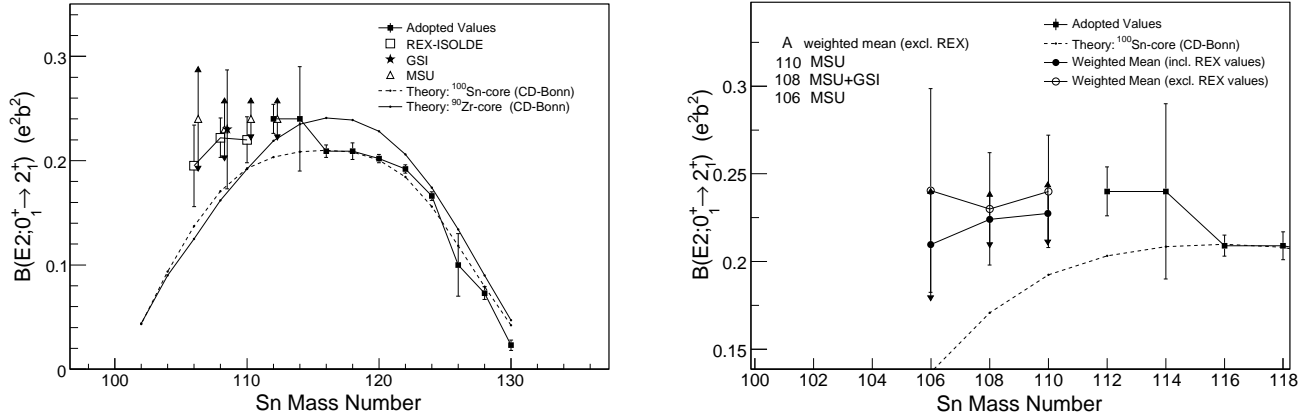


FIG. 3: Left panel; experimental and theoretical  $B(E2)$  values. The dashed curve represents the result from a shell model calculation using  $^{100}\text{Sn}$  as core and a  $\nu(g_{7/2}, d, s, h_{11/2})$  model space with a neutron effective charge  $e_{eff}^\nu = 1.0e$ . The solid line corresponds to using  $^{90}\text{Zr}$  as core and a  $\pi(g, d, s)-\nu(g_{7/2}, d, s, h_{11/2})$  model space with  $e_{eff}^\nu = 0.5e$ . Right panel; weighted mean  $B(E2)$  values for the  $^{106,108,110}\text{Sn}$  isotopes. Filled circles represent the weighted mean values including the REX result. See the text for details.

The relative purity of the low-energy excited states in the even-mass Sn isotopes make them suitable for a shell-model analysis. The relevant model space for neutrons and protons outside of the  $^{100}\text{Sn}$  core consists of the  $1d_{5/2}0g_{7/2}2s_{1/2}1d_{3/2}0h_{11/2}$  orbits. The first orbit immediately below the  $N = Z = 50$  shell gap is  $0g_{9/2}$ . It is natural to assume that the missing  $0_{gs}^+ \rightarrow 2_1^+$  transition strength, for the  $^{100}\text{Sn}$  core calculation (see Fig. 3), can partly be accounted for by proton core-excitations. Similarly, neutron excitations across the shell-gap would also increase the  $E2$  strength. These excitations would be enhanced by a strong  $E2$  coupling between the  $0g_{9/2}$  and  $1d_{5/2}$  orbits. Since the  $0g_{7/2}1d_{5/2}$  orbits start to dominate the configurations with a decreasing number of neutrons outside the core the available phase space for excitations of this kind increases. However, as the experimental  $B(E2; 0_{gs}^+ \rightarrow 2_1^+)$  increases already when going from  $^{116}\text{Sn}$  to  $^{114}\text{Sn}$  it appears that proton excitations play an important role in the transition. A shell-model

calculation based on an extended model space that includes a limited number of  $0g_{9/2}$  protons and neutrons is on the verge of computational feasibility. It should be noted that a coupling to orbits outside of the model space is approximately accounted for in many-body theory by the perturbative construction of the effective interaction [16]. Previous calculations based on a  $^{100}\text{Sn}$  core indicated the need for an explicitly expanded model space. Banu et al. [1] included this effect up to  $4p - 4h$  proton core-excitations by means of a seniority truncated interaction outside of a  $^{90}\text{Zr}$  core. Due to the seniority truncation in that calculation the symmetric trend of the  $B(E2)$  values were retained. The impact of core-excitations on the  $0_{gs}^+ \rightarrow 2_1^+$  transition probability depends in part on the  $0g_{9/2} - 1d_{5/2}$  energy separation,  $E_g$ . In a limited  $0g_{9/2}1d_{5/2}$  neutron model space a  $\sim 50\%$  increase of the  $B(E2)$  can be noted with a  $\sim 50\%$  reduction of  $E_g$  from 6 MeV to 3 MeV. Neither the proton nor the neutron  $0g_{9/2}^{-1}1d_{5/2}$  coupling strength is known from

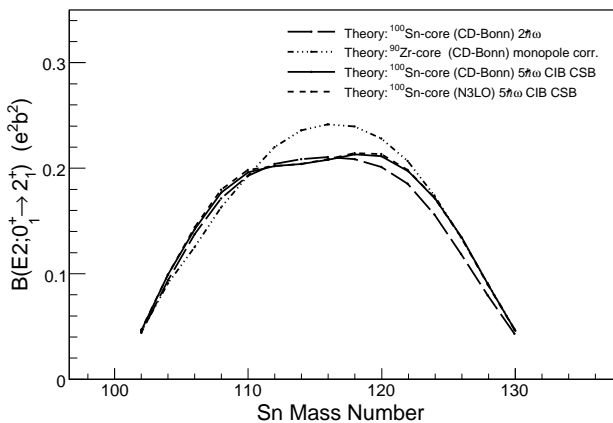


FIG. 4: Theoretical  $B(E2)$  values given in  $e^2b^2$  for the even Sn isotopes. The first two calculations are identical to the ones presented in Fig. 3. The  $^{90}\text{Zr}$  core calculation was seniority truncated and based on a monopole corrected CD-Bonn interaction [1]. The remaining calculations are based either on the N3LO interaction or a more recent CD-Bonn interaction. The number of excitations allowed in the perturbative scheme is here  $5\hbar\omega$ . Whether the interaction incorporated charge symmetry breaking (CSB) and charge independence breaking (CIB) is indicated in the legend.

experiment. The so-called monopole drift of the single-particle orbits can play a key role in self-conjugate nuclei. It was shown in Ref. [17] that the interaction between neutrons and protons in  $j = \ell \pm 1/2$  orbits modify the effective single particle energies, as observed for instance in [18]. With this line of reasoning, the neutron-deficient Sn isotopes could exhibit a tendency for the proton  $0g_{9/2}$  to become less bound as the number of neutrons in  $0g_{7/2}$  decreases. This type of single-particle drift was also observed in the Zr ( $Z = 40$ ) isotopes as pointed out in Ref. [19]. Further experimental evidence for monopole drift along isotone chains come from  $(d, p)$ , and  $(d, t)$  reactions [20]. Experimental analysis of isomeric core excited states in  $^{98}\text{Cd}$  gives a  $^{100}\text{Sn}$  shell gap of  $\sim 6.5$  MeV for both neutrons and protons [21]. In a similar

fashion the energy of the  $25/2^+$  level, with a dominating  $\nu 0g_{9/2}^{-1}$  component, in  $^{99}\text{Cd}$  points towards a shell gap of the same size [22]. However, recent experimental results concerning the three first excited states in the  $N = Z + 2$  nucleus  $^{110}\text{Xe}$  instead point towards a possible weakening of the  $N = Z = 50$  shell closure [23]. Clearly, a strong shell-closure is only consistent with the experimental data presented here if the above mentioned core excitations can be proven to account for the enhanced transition strength. For this paper we have expanded the shell-model calculations in Ref. [1] by using two more recent nucleon-nucleon interactions (see Fig. 4). One, based on chiral effective field theory, N3LO [24], includes pions and nucleons as the only effective degrees of freedom. The other one is a more recent type of CD-Bonn interaction [25]. In contrast to the calculations in Ref. [1] these two interactions include Coulomb effects and explicitly break the charge symmetry and charge independence between the nucleons. The divergent two-body matrix elements were renormalized using G-matrix theory [16] and subsequently tailored to the model space using many-body perturbation techniques [16]. Interaction terms of two-body matrix elements up to third order were included in this treatment and the maximum energy of intermediate excitations was increased to a limit of  $5\hbar\omega$ . As can be seen in Fig. 4 the trend of the  $B(E2)$  values is sensitive to the coupling to orbits outside of the model space. In particular, the calculations now show an interesting deviation from the symmetry expected in the seniority model.

In this paper we have reported on Coulomb excitation experiments using  $^{108,106}\text{Sn}$  beams at REX-ISOLDE. With this the  $B(E2)$  systematics now extend down to  $^{106}\text{Sn}$ . Calculations using the N3LO nucleon-nucleon interaction and a recent CD-Bonn interaction show an interesting deviation from the symmetric trend predicted by the seniority model but still do not reproduce the experimental data. This shows the need for further theoretical investigations of the microscopic description of the nucleon-nucleon interaction as applied to the  $^{100}\text{Sn}$  shell closure. This work was supported by the European Union through RII3-EURONS (Contract No. 506065).

- 
- [1] A. Banu *et al.* Phys. Rev. C **72**, 061305(R) (2005).  
[2] J. Cederkall *et al.* Phys. Rev. Lett. **98**, 172501 (2007).  
[3] C. Vaman *et al.* Phys. Rev. Lett. **99**, 162501 (2007).  
[4] I. Talmi, Nucl. Phys A **172**, 1 (1971).  
[5] J. N. Orce *et al.* Phys. Rev. C **76**, 021302(R) (2007).  
[6] O. Kester *et al.* NIM B**204**, 20-30 (2003).  
[7] BNL Evaluated Nuclear Structure Data File (ENSDF)  
[8] F. Wenander. Nucl. Phys. A **701**, 528-536 (2002).  
[9] D. Cline Bull. Am. Phys. Soc. **14:726** (1969).  
[10] P. Reiter *et al.* Nucl. Phys. A **701**, 209-212 (2002).  
[11] A. N. Ostrowski *et al.* NIM A **480** 448 (2002).  
[12] A. Ekström *et al.* to be published.  
[13] T. Czornyka *et al.* Am Phys. Soc. **28:745** (1983).  
[14] R. Graetzer *et al.* Phys. Rev. C **12**, 1462 (1975).  
[15] D. Seweryniak *et al.* Nucl. Phys **A**, 589, 175-200, (1995)  
[16] M. Hjorth-Jensen *et al.*, Phys. Rep. **261**, 125 (1995).  
[17] T. Otsuka *et al.* Phys. Rev. Lett. **95**, 232502 (2005).  
[18] L. Gaudefroy *et al.* Phys. Rev. Lett. **97**, 092501 (2006).  
[19] P. Federman and S. Pittel Phys. Rev. C **20**, 820 (1979).  
[20] B. L. Cohen *et al.* Phys. Rev. **127**, 1678 (1962).  
[21] A. Blazhev *et al.* Phys. Rev. C **69**, 064304 (2004).  
[22] D.J. Dean *et al.* Prog. in Part. and Nucl. Phys. **53** 419-500 (2004).  
[23] M. Sandzelius *et al.* Phys. Rev. Lett. **99**, 022501 (2007).  
[24] D. R. Entem *et al.* Phys. Rev. C **68**, 041001 (2003).  
[25] R. Machleidt *et al.* Phys. Rev. C **63**, 024001 (2001).